

# Timing of the brain events underlying access to consciousness during the attentional blink

Claire Sergent<sup>1</sup>, Sylvain Baillet<sup>2</sup> & Stanislas Dehaene<sup>1</sup>

**In the phenomenon of attentional blink, identical visual stimuli are sometimes fully perceived and sometimes not detected at all. This phenomenon thus provides an optimal situation to study the fate of stimuli not consciously perceived and the differences between conscious and nonconscious processing. We correlated behavioral visibility ratings and recordings of event-related potentials to study the temporal dynamics of access to consciousness. Intact early potentials (P1 and N1) were evoked by unseen words, suggesting that these brain events are not the primary correlates of conscious perception. However, we observed a rapid divergence around 270 ms, after which several brain events were evoked solely by seen words. Thus, we suggest that the transition toward access to consciousness relates to the optional triggering of a late wave of activation that spreads through a distributed network of cortical association areas.**

A central question in the study of conscious perception relates to the neural basis of conscious access: what are the neural processes that allow stimulus information to become available for explicit report? Imaging studies have shown that conscious access is accompanied both by increased activity in perceptual areas<sup>1–5</sup> and by the specific involvement of a largely distributed frontoparietal network with increased functional connectivity<sup>1,6–8</sup>. Which of those observed effects corresponds to the primary correlates of conscious access? According to some authors, the difference between conscious and nonconscious processing primarily resides in different levels of activation in early stimulus-specific areas<sup>4,9</sup>. Others, however, emphasize that these early events can also be observed under nonconscious conditions<sup>1,6</sup> and therefore suggest that the critical correlate of conscious access is a late, optional triggering of a ‘second stage’ of processing involving a distributed frontoparietal network<sup>10–12</sup>.

To disentangle theories predicting an early, gradual correlate of conscious access and theories predicting late divergences, we took advantage of the temporal resolution afforded by event-related potentials (ERP) in an attentional blink experiment<sup>13,14</sup>. In this procedure, two masked visual targets are presented successively. For short stimulus onset asynchrony (SOA) between both targets (200 to 500 ms), identification of the first target (T1) hinders the detection of the second target (T2), although T2 is easily seen when no task on T1 is required. The attentional blink provides an ideal situation in which identical stimuli lead to different conscious reports. Indeed, in previous experiments in which we asked participants to rate the visibility of a target word (T2) on a continuous scale, we showed that during the attentional blink, T2 was sometimes fully perceived but sometimes not detected at all<sup>15</sup>. In the present ERP study, we searched for the neural events underlying this bimodal distribution of conscious reports.

Previous ERP studies of the attentional blink<sup>16–18</sup> examined only specific ERP components and their preservation or elimination during the attentional blink. By contrast, here we were able to examine the complete temporal sequence of brain events leading to conscious access. We achieved this by comparing trials in which the target word T2 was present (whether it was seen or unseen) with trials in which it was absent and replaced by a blank screen.

## RESULTS

### Bimodal distribution of conscious reports

We used a short (258 ms) and a long (688 ms) SOA between T1 and T2. We used two task conditions: single task (subjects were asked to respond to T2 only) and dual task (subjects were asked to respond to both T2 and T1; see **Fig. 1** for summary of attentional blink procedure). T2 was a number word and could be either present or absent; in the latter case, the word was simply replaced by a blank screen. The task on T2, performed shortly after T2 was presented, was to rate its visibility on a continuous scale (see Methods).

Mean subjective visibility on the scale showed a classical attentional blink pattern (**Fig. 1**): when T2 was present, mean visibility dropped markedly at short T1–T2 SOA only when participants had to perform a task on T1 (task by SOA interaction:  $F_{1,15} = 62.5$ ;  $P < 0.0001$ ). When T2 was absent, responses on the scale were all grouped towards the lowest visibility degree in all conditions. When T2 was present in the single-task condition, responses were all grouped towards high-visibility degrees. However, during the attentional blink (dual task, short SOA), a very different, bimodal pattern was observed: on some trials, participants gave high visibility ratings, close to those obtained outside the attentional blink, whereas on the others, they used the lowest visibility ratings (24.8% of the responses at 0% visibility; **Fig. 1**). We

<sup>1</sup>Institut National de la Santé et de la Recherche Médicale Unité 562, Cognitive Neuroimaging, Service Hospitalier Frédéric Joliot, Commissariat à l’Energie Atomique, 4, place du Général Leclerc, 91401 Orsay Cedex, France. <sup>2</sup>Cognitive Neuroscience and Brain Imaging Laboratory, Centre National de la Recherche Scientifique UPR 640-LENA, Hôpital de la Salpêtrière, 47, boulevard de l’Hôpital 75651 Paris Cedex 13, France. Correspondence should be addressed to C.S. (sergent@shfj.cea.fr).

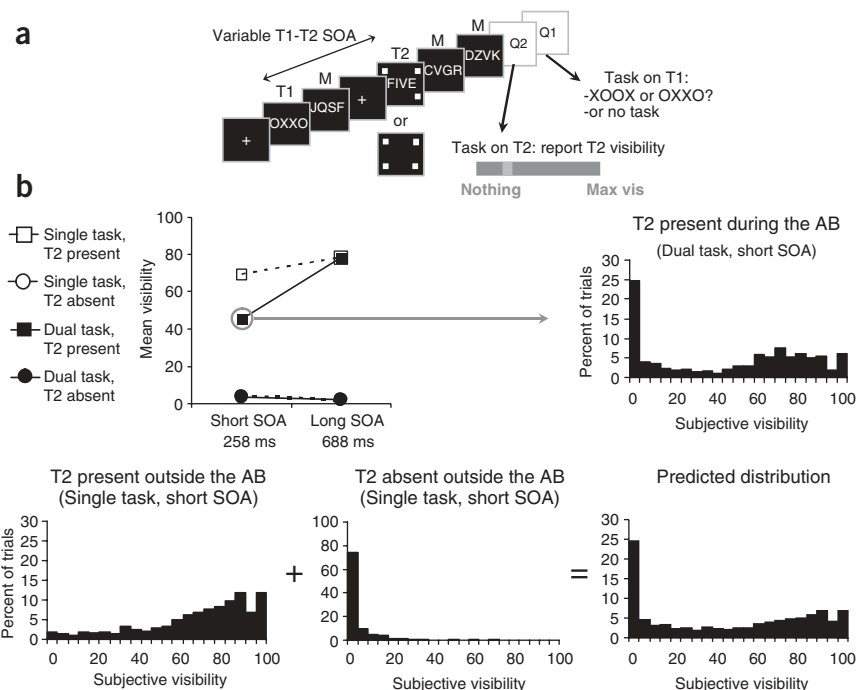


**Figure 1** Experimental protocol and behavioral results recorded during the ERP session. **(a)** Each trial consisted of a simple sequence containing five items: T1 followed by a mask (M) and T2 (which could be present or absent) followed by two successive masks. The SOA between T1 and T2 could be either short (258 ms) or long (688 ms). Presentation of T2 was signaled by four surrounding squares. When T2 was absent, the four squares were presented on a blank screen. Each trial ended with a question on the visibility of T2 (Q2: visibility scale) using a cursor (small rectangle on the scale) and, in the dual-task condition, a question on T1 (Q1). In the actual experiment, T2, when present, was a French number word. **(b)** Upper left graph shows mean subjective visibility of T2 rated on a scale in the various experimental conditions. Upper right graph shows response distribution in the ‘critical blink’ condition. A combination of the response distributions observed for ‘T2 present’ and ‘T2 absent’ outside the attentional blink (AB) predicted a response distribution that accounted for 97% of the variance in the observed response distribution during the attentional blink (bottom row).

performed a multiple linear regression of this response distribution using as predictors the distributions obtained outside the attentional blink (single task, short SOA) when T2 was present and when T2 was absent (Fig. 1). This regression accounted for 96.9% of the data, with significant contribution of both predictors ( $P$  values < 0.001). Thus, we could interpret the responses obtained during the attentional blink as being a mixture of ‘seen’ and ‘unseen’ states.

We also observed a slight decrease in visibility ratings within the ‘seen’ trials. Both this small decrease and the jump towards zero visibility replicate our previous observations<sup>15</sup> and can be well captured by a dynamical phase transition model<sup>19–21</sup>. Control experiments<sup>15</sup> showed that when the duration of the target was varied, participants were able to use the response scale continuously to signal small changes in their perception. Thus, the bimodal blink pattern is unlikely to be due to an inability to use the scale, but rather is likely to faithfully reflect a failure of subjective perception of T2 on some ‘blinked’ trials; that is, trials in which the attentional blink effectively prevented the perception of T2.

### The neural fate of ‘blinked’ and seen stimuli

In order to analyze the brain events underlying this bimodal distribution, we compared the ERPs evoked by T2 during the attentional blink (short SOA, dual task) when T2 was seen and when it was not seen (empirically defined as visibility  $\geq$  or < 50%). Because T1 and the masks also evoked ERPs, we extracted the potentials specifically evoked by T2 by subtracting the ERPs evoked when T2 was absent and replaced by a blank screen (Supplementary Fig. 1). Supplementary Video 1 shows the complete sequence of events evoked by seen and unseen T2s (see also Figs. 2–5 and Supplementary Table 1). We did not observe any significant difference in the early visual P1 and N1 waves (96 and 180 ms) evoked by seen and unseen T2s, either in amplitude or in topography (Fig. 2). Then, the ERPs evoked by seen and unseen words showed a series of diverging events. The first difference was observed around 170 ms, with a slightly stronger positivity over central electrodes for seen T2s. A larger divergence occurred around 270 ms, when seen

T2s evoked a stronger left-lateralized posterior negativity (N2, 276 ms) followed by a more anterior negativity (N3, 300 ms) that was absent for unseen T2s (Fig. 3). Two subsequent waveforms (P3a, 436 ms; late P3b, 576 ms) were also present only when T2 was seen (Fig. 5).

However, processing of unseen T2s did not stop at the time when ERPs evoked by seen T2s began to diverge. Even after 270 ms, some waveforms still showed reduced but significant activity for unseen T2s. Seen T2s evoked a central negativity (N4, 348 ms) that was also present when T2 was not seen, with a similar topography but reduced intensity (Fig. 4). Similarly, a central positivity (early P3b, around 480 ms) was transiently evoked by both seen and unseen T2s (significant for 32 ms).

Although our primary goal was to study the temporal dynamics of access to consciousness, our high-density ERP recordings allowed some tentative inferences about the cerebral localization of the underlying generators. A model of distributed cortical sources (see Methods) allowed us to display, at each time step, the putative distribution of activity on the inflated cortical surface (Figs. 2–5) and to reconstruct the temporal profile of activation of reconstructed sources at various cortical locations (Fig. 6). Up to about 200 ms, activation unfolded identically for seen and unseen T2s over the right occipital and then the bilateral occipitotemporal regions. Activation then expanded anteriorly into the left temporal lobe and inferior frontal regions, where we observed a surge of activation and a progressive divergence between seen and unseen T2s. This divergence reached its maximum by about 300 ms. Elevated and durable activations (lasting ~200 to 300 ms) were then observed in bilateral dorsolateral prefrontal, ventral prefrontal and anterior cingulate regions, and, to a lesser extent, inferior parietal cortex, specifically when T2 was seen. Finally, in the late part of the epoch, frontoparietal activity remained in the right hemisphere, whereas we observed a late left-lateralized reactivation in posterior cortices.

### Neural events correlating with bimodal conscious report

We further investigated the relation between ERP events and the visibility ratings by further subdividing the trials into four

categories of visibility ratings. Our goal was to identify which events varied linearly with the ratings and which showed a nonlinear change related to the bimodal character of the response distribution (Fig. 7; see Methods).

The results confirmed that the ERPs evoked by T2 started to show significant changes as a function of visibility from around 270 ms onward. By contrast, early P1 and N1 waves (96 and 180 ms) were not significantly affected. This was particularly notable for the strong N1 wave, which was unchanged whether T2 visibility was rated with the highest or the lowest scores on the scale.

The intensity of the N2 wave decreased linearly with reduced T2 visibility. By contrast, the N3, P3a and late P3b waves showed a nonlinear relation to visibility. They were present only when T2 visibility was above 50%, whereas below 50% visibility, T2 did not

evoke any significant activity in comparison to 'T2 absent' trials (all values of  $F_{1,12} < 1$ ). These waves thus showed a major change around 50% visibility, matching the bimodal character of the visibility ratings.

This analysis also confirmed that the N4 wave was reduced, but not suppressed, with reduced visibility, and that nonconscious processing went on after conscious and nonconscious processing had diverged.

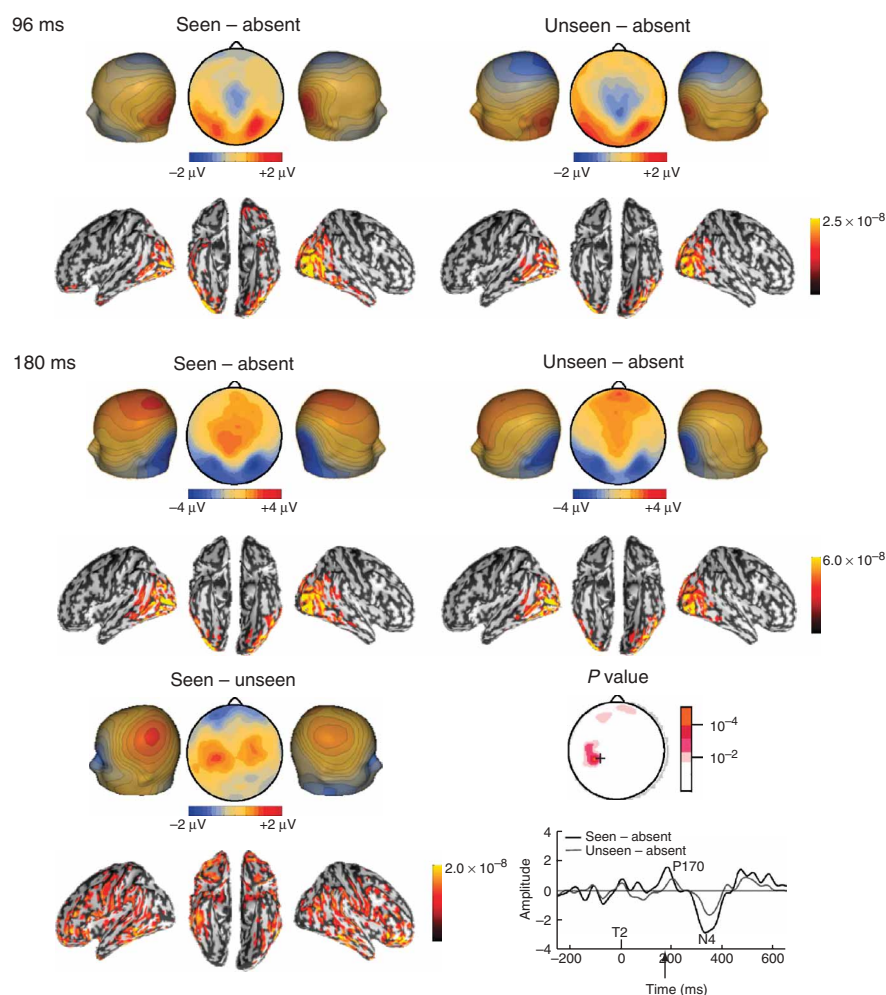
### Causes of the blink: ERPs evoked by the task on T1

Why is the same T2 sometimes perceived and sometimes not seen? Two-stage models of the attentional blink postulate that during the attentional blink, T2 processing is denied access to a second processing stage, with a limited capacity, that is used to process T1 (ref. 22). To investigate which neural events correspond to this second stage and

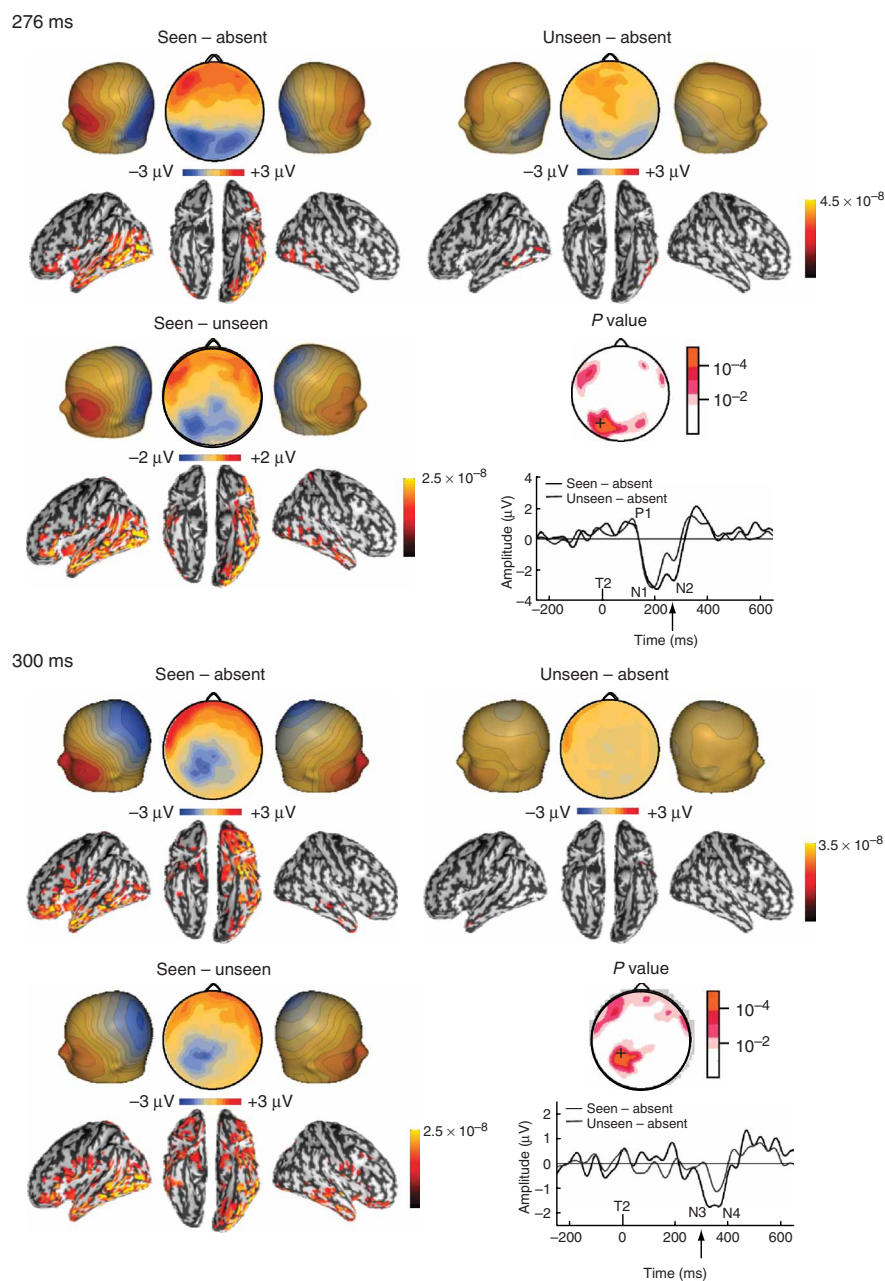
might cause the attentional blink, we contrasted the ERPs evoked by T1 when participants did or did not perform the T1 task. This contrast probably includes both processing of T1 itself and processing related to the task switch between T1 and T2. Although this contrast affected even the earliest ERPs evoked by T1 (P1, N1), its main effect was to generate or strongly enhance a sequence of later waveforms (Fig. 8a): a left-lateralized posterior negativity (N2,  $F_{1,15} = 47.86$ ;  $P < 0.0001$ ), an anterior positivity (P3a,  $F_{1,15} = 47.81$ ;  $P < 0.0001$ ) and a posterior positivity (P3b,  $F_{1,15} = 60.71$ ;  $P < 0.0001$ ). Thus, the presence of the T1 task, which causes the blink, seemed to affect principally the same processing stages (indexed by the N2, P3a and P3b waves) that were also found to be involved in conscious access to T2.

Figure 8a illustrates the temporal relation between the ERPs induced by the task on T1 and those evoked by T2. The early T2-induced waveforms (P1 and N1), which were not affected by the blink, coincided with the P3a and early P3b evoked by the task on T1, thus indicating that these waveforms index non-conflicting processing stages that can proceed in parallel. However, the divergence between seen and unseen T2s at 270–300 ms coincided with the end of the late P3b evoked by the T1 task. This temporal coincidence suggests that the attentional blink might arise from a competition between the late part of the P3b induced by the task on T1 and the N2 wave evoked by T2.

We further investigated the trial-by-trial relation between those components as a function of T2 visibility (Fig. 8b; see Methods). The T2-evoked N2 did indeed overlap in time with the late part of the T1-evoked P3b (Fig. 8b), and the intensity of the N3 was reduced with reduced visibility. Furthermore, when T2 was seen, the T1-evoked P3b seemed to reach its peak earlier in time and then decreased at a faster rate. This was confirmed by a direct comparison of T1-evoked P3b amplitude over an early time window



**Figure 2** Preservation of initial visual processing steps during the attentional blink. Voltage scalp maps show activation evoked by T2 during the attentional blink (dual task, short SOA) as a difference between seen minus absent, unseen minus absent and seen minus unseen conditions at different time points after T2 onset (P1, peaking at 96 ms; top row; N1, peaking at 180 ms; bottom rows). Below each voltage map, a cortical current map accounting for the observed topography is represented on a smoothed version of the standardized cortex (see Methods) in three different views: left view, ventral view (middle image) and right view. Activations are expressed in terms of dipole current amplitude (A-m), with a threshold at 50% of the maximal value indicated on the scale. Electrode sites where the seen minus unseen difference was significant at  $P \leq 10^{-2}$  ( $t$ -test for the 180 ms sample) are represented on the 'P value' scalp map. Graph at lower right shows the time course of the voltage recorded at a left central electrode site (indicated by a cross on the 'P value' map). The arrow on the time axis indicates 180 ms.



**Figure 3** First large divergences between conscious and nonconscious processing during the attentional blink. The N2 wave peaked at 276 ms (top rows). The associated graph shows the time course of the voltage recorded at a left posterior electrode site (indicated by a cross on the 'P value' map). The arrow on the time axis indicates 276 ms. The subsequent N3 wave peaked at 300 ms (bottom rows). The associated graph shows the time course of the voltage recorded at a central electrode site (indicated by a cross on the 'P value' map). The arrow on the time axis indicates 300 ms. Other conventions as in **Figure 2**.

(100–200 ms after T2), which indicated that the P3b was more intense over this early time period in trials in which T2 would later be seen ( $t_{1,087} = 3.4$ ;  $P < 0.001$ ). Conversely, over a later time window (204–300 ms after T2), the P3b amplitude was slightly greater on trials where T2 would later be missed ( $t_{1,087} = 2.2$ ;  $P < 0.05$ ). Thus, it is possible that that trial-to-trial variability in the duration and/or difficulty of the T1 task and/or the task switching process creates fluctuations in the amplitude of the late part of the T1-evoked P3b, thus affecting the severity of the competition between T1 and T2 (as reflected in

the strength of the T2-evoked N2) and occasionally denying conscious access to T2.

## DISCUSSION

### Early visual events and consciousness

According to some authors, the difference between conscious and nonconscious processing primarily resides in different levels of activation in early stimulus-specific areas<sup>4,9</sup>. Along with previous findings on the attentional blink, our results argue against this view. Using separate experiments to isolate specific waveforms, previous ERP studies of the attentional blink<sup>16–18,23</sup> have shown that the P1, N1 and N400 waveforms can be preserved during the attentional blink, whereas a late P300 component is eliminated<sup>16,17</sup>. The present study goes beyond these findings by using a more global subtraction (T2 present versus T2 absent), which allows us to extract, in a single experiment, the complete cascade of events evoked by T2, whether seen or unseen.

Previous studies have shown that the early visual P1 and N1 waves evoked by a probe flash concomitant to the presentation of T2 (a letter) are preserved during the period where T2 report is affected by the attentional blink<sup>17</sup>. However, this previous experiment did not assess consciousness of the flash and did not measure ERPs evoked by T2 itself. In particular, one could not exclude the possibility that although an attentional blink is observed for the T2 letter, the concomitant probe flash actually escapes the attentional blink, as it is a salient, unmasked event. The present experiment extends this previous finding by providing direct evidence that the P1 and N1 waves evoked by T2 itself are completely preserved whether T2 is seen or not seen during the attentional blink.

Previous studies have also shown that 'blinked' stimuli can reach surprisingly high levels of analysis<sup>7,16,24</sup>. In two separate experiments, others have demonstrated that the N400 evoked by semantic mismatch is completely preserved during the attentional blink<sup>16,17</sup>, whereas the P300 (evoked by the occurrence of infrequent targets) is suppressed<sup>17</sup>. These results suggest that although stimuli can be processed up to a level of semantic analysis during the attentional

blink, the attentional blink affects another late stage of processing, presumably consolidation of target representation into working memory. The general subtraction used in the present study allowed us to assess the relative timing of events surrounding the first divergence between seen and unseen ERPs and, in particular, to provide direct evidence that late ERPs evoked by unseen T2s (N4) could indeed occur after this first divergence.

The finding of preserved early visual processing for nonconscious targets during the attentional blink contrasts with another study<sup>9</sup>

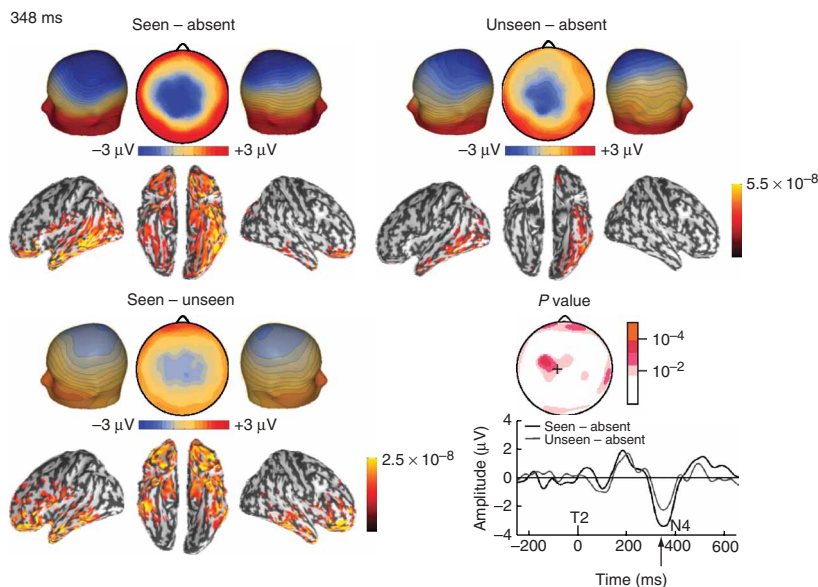


**Figure 4** Reduced amplitude of a late central negativity on nonconscious trials during the attentional blink. The N4 (a central negativity) peaked at 348 ms. The associated graph shows the time course of the voltage recorded at a central electrode site (indicated by a cross on the ‘P value’ map). The arrow on the time axis indicates 348 ms. Other conventions as in **Figure 2**.

showing that for identical low-contrast grating patches presented at the subject’s threshold, the evoked P1 wave is larger when the patch is detected than when it is missed. While differences were also observed in later components (N2, P3), they were assumed to merely reflect the consequences of this initial difference. Thus, the authors concluded that the P1 is the primary correlate of consciousness and that later waves do not contribute directly to conscious perception<sup>9</sup>. Our results are inconsistent with this model and suggest a different interpretation. When visual stimuli are degraded and close to threshold, as in this previous study<sup>9</sup>, stochastic variations in P1 amplitude might be sufficient to occasionally prevent conscious access. However, in the attentional blink procedure, where the stimuli are highly contrasted and undegraded, our results show that they can generate strong P1 and N1 components in the absence of conscious report and indicate that only the late components correlate with conscious access.

An alternative interpretation of the diverging results is that conscious perception of simple grating patches resides in early visual processing (for instance, in extrastriate cortex), whereas consciousness of more complex stimuli such as words resides in higher-level areas. However, we consider this interpretation unlikely. Although T2 was a word, our subjects were merely asked to detect the presence of any stimulus at the time of T2 presentation, which was clearly signaled by a display of surrounding squares (**Fig. 1**). Furthermore, shortly afterwards, subjects were given the opportunity to report any degree of perception of T2. If subjects had any feeling of having seen T2, they were told to use a nonzero visibility rating (see Methods). In spite of these methodological precautions, subjects frequently used the zero-visibility category during the blink. The fact that even in this case the P1 and N1 were unaffected strongly suggests that early visual processing is not sufficient by itself to create a conscious percept.

This conclusion is corroborated by many observations of visual processing of nonconscious stimuli in occipitotemporal cortex during masking<sup>1,25</sup>, neglect<sup>6</sup>, attentional blink<sup>7,26</sup> or inattention<sup>8</sup>. Electrophysiological recordings in the macaque area V1 confirm that early visual

activation can be fully preserved on trials in which the animal reports no perception<sup>27,28</sup>. Only in a second phase (>100 ms) are differential activations of V1 observed for seen versus unseen trials<sup>27</sup>, presumably due to top-down inputs from other areas. Such late amplification is likely to contribute to observations of correlation of V1 activity with consciousness using non-time-resolved methods such as fMRI (functional magnetic resonance imaging)<sup>29</sup>.

### Two stages of stimulus processing

Along with previous observations<sup>7,17,30</sup>, our data seem consistent with a two-stage model of the attentional blink<sup>22</sup> according to which T2, when ‘blinked’, receives normal perceptual processing but is prevented from accessing a second capacity-limited stage which is already engaged by T1 processing. Our present results help characterize the transition towards second-stage processing in space and time. Indeed, this transition seems to correspond to an intermediate period of fast dynamical divergence (170–300 ms after T2), after which most waveforms acquired a bimodal character

(being either present or absent), which is ultimately reflected in behavioral subjective reports. Our present findings also provide direct evidence that processing of stimuli that are denied access to the second stage is not abruptly stopped at the time of the bottleneck but can continue for a long time within the left temporal lobe. Thus, conscious and nonconscious processing can proceed along partially distinct and parallel anatomical pathways, and their time courses may overlap.

Can the present recordings be used to specify which brain areas are concerned with the ‘second stage’ of stimulus processing? We emphasize that the ERP methodology cannot be used to make unambiguous inferences about brain localization. Nevertheless, high-density recordings do provide some indicative evidence about localization, which was extracted here by using a model of distributed cortical sources. This source model indicated that seen words initially gained an edge over unseen words within left temporal and inferior frontal regions (~300 ms), followed by an intense spread of activation to lateral prefrontal and anterior cingulate cortices (~440 ms) and finally extending again to posterior regions (~580 ms).

Consistent with these results, two recent MEG studies of normal word reading indicate that, shortly after initial occipitotemporal processing, word-induced activation<sup>31</sup> and word repetition effects<sup>32</sup> can be observed in the left inferior Rolandic cortex about 200–250 ms after the stimulus, preceding a rapid expansion of activity to a large portion of the left and right temporal lobes<sup>31,32</sup>. Furthermore, compatible with our putative generators, previous studies of the attentional blink using fMRI<sup>7,26,33</sup> and magnetoencephalography (MEG)<sup>34</sup> have found anterior cingulate, lateral prefrontal and parietal regions to be more active in seen trials than in ‘blinked’ trials. Spectral methods have shown a synchronization of brain activity in the beta frequency band (13–18 Hz) across distributed frontal, parietal, cingulate and anterior temporal regions<sup>34</sup> in the same time window where we observed the P3a and P3b (about 500 ms post-stimulus). This synchronization was considerably reduced on ‘blinked’ trials and was thought to index synchronous target detection, visual attention and working memory processes<sup>34</sup>. Intracranial

studies<sup>35</sup> further confirm that the P3 relates to the activation of distributed cerebral regions, dominated by associative parietal and frontal areas.

Overall, our results are consistent with models that attribute an important role to distributed prefrontal, parietal and cingulate activity in relation to conscious perception, as also observed in phenomena such as binocular rivalry<sup>36</sup>, inattentive blindness<sup>37</sup>, change blindness<sup>8</sup> or masking<sup>1</sup>.

The involvement of these regions is consistent with recent simulations of a 'global neuronal workspace' model<sup>10</sup> according to which suprathreshold stimuli gain access to consciousness by mobilizing a global workspace<sup>11</sup> of multiple distant associative areas including prefrontal, parietal and anterior cingulate nodes, which in turn send top-down amplification signals to stimulus-encoding processors in visual regions<sup>19,21</sup>. The reverberant activation would be reflected in electroencephalograms (EEG) both by the P3 and high-frequency synchronization<sup>19,21</sup>. The source model of the P3b obtained in the present experiment shows a late reactivation of occipital areas, suggesting top-down amplification. This model also predicts the existence of a discontinuous threshold for conscious access<sup>15,19,21</sup>, a phenomenon generally observed for nonlinear autoamplified systems<sup>20,38</sup>. We propose that the present findings could indicate the existence of such a sharp bifurcation. Although a gradual reduction in the intensity of some waves (such as N2 and N4) seems to account for a gradual change in the perception of the target word (as reflected in variable visibility ratings in the seen trials), whether this perception is available for conscious report seems to depend mostly on the optional triggering of 'bimodal' waves (such as N3, P3a and P3b) that match the bimodal distribution of visibility ratings.

### Causes of the blink: competition between two targets

So far, few studies have investigated the neural causes of the attentional blink<sup>23,30</sup>. fMRI has been used to show that increasing the attentional demands of the T1 task, which increases the attentional blink, yields stronger activation in the right intraparietal sulcus, the anterior cingulate and right frontal cortex<sup>30</sup>. This suggests that the capacity-limited stage responsible for the attentional blink involves a network of parietal and frontal areas. In the present study, we have directly investigated the effect of the principal parameter determining the attentional blink: the presence or absence of a task on T1. The T1 task particularly affects ERP components similar to those correlating with conscious access to T2, namely N2, P3a and P3b. This observation supports the idea that these components index a capacity-limited stage capable of processing only one task at a time. It is consistent with

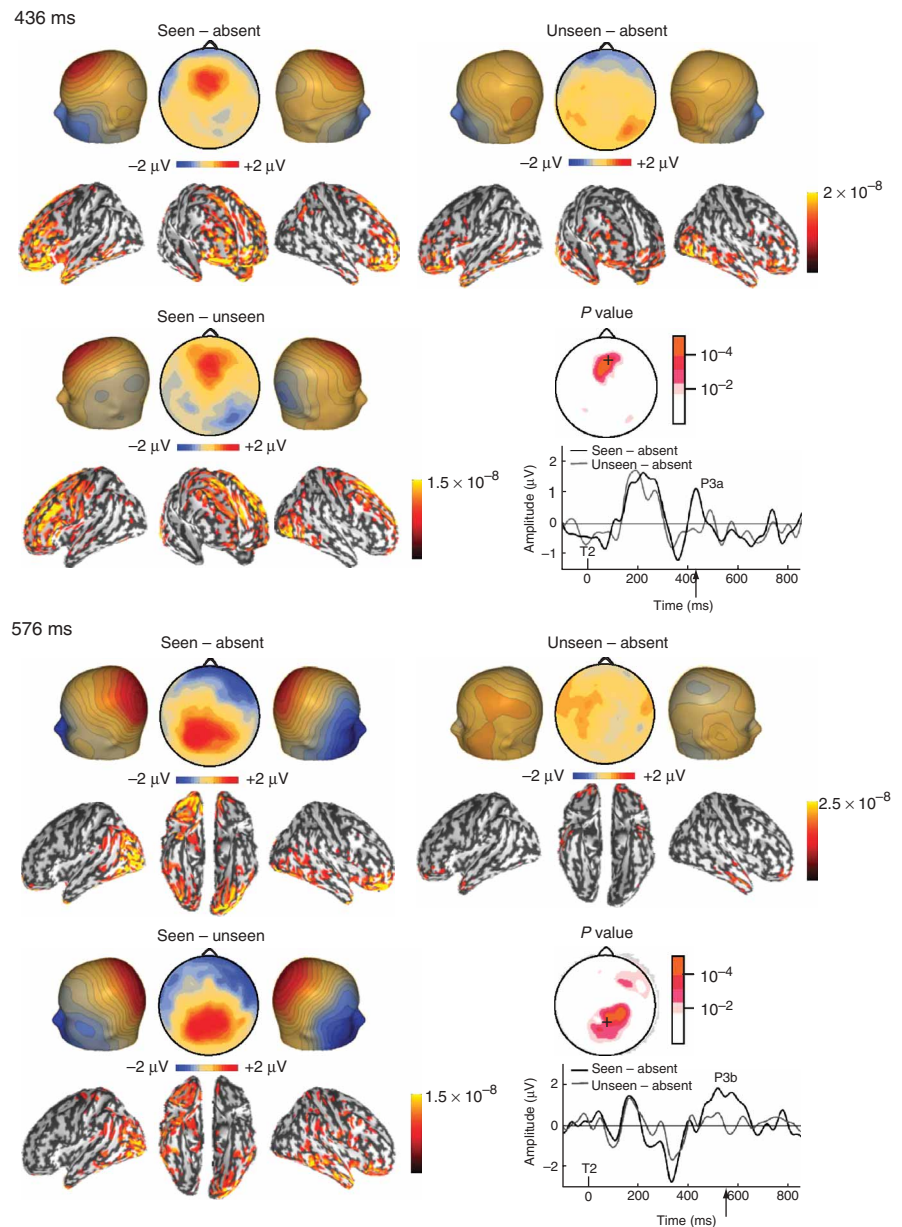
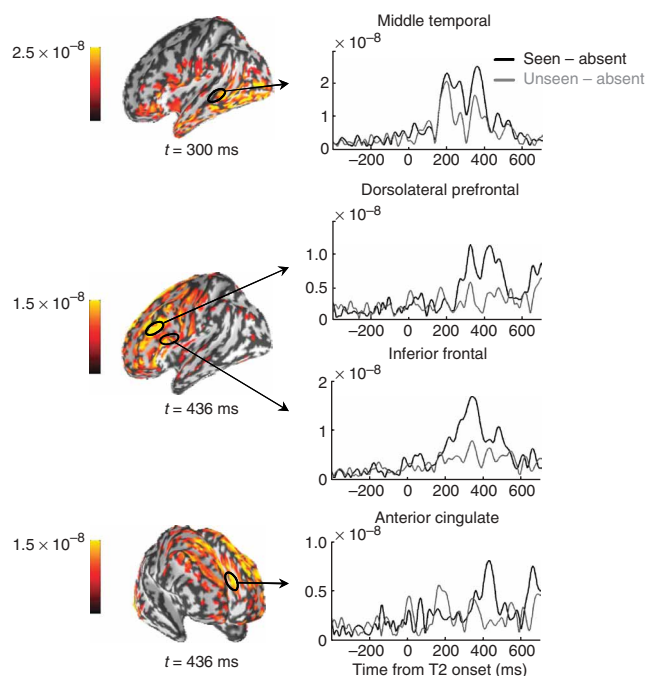


**Figure 5** Late positive complex exclusively evoked by seen T2s during the attentional blink. The P3a (a late frontal positivity) peaked at 436 ms (top rows) and the late P3b (a late parietal positivity) peaked at 576 ms (bottom rows) were exclusively evoked by seen T2s. The associated graphs show the time courses of the voltage recorded at frontal (top) and parietal (bottom) electrode sites. Below each voltage map, a cortical current map accounting for the observed topography is represented on a smoothed version of the standardized cortex (see Methods). For the P3a wave (436 ms), the middle image is a frontal view which shows, among other activations, an activation in the anterior cingulate when T2 was seen. For the late P3b wave (576 ms), the middle image corresponds to a ventral view. Other conventions as in **Figure 2**.

previous ERP results showing a reciprocal relationship between the size of the P3 waves evoked by two concurrent tasks<sup>39</sup>.

On the basis of an analysis of the temporal coincidence of these components (**Fig. 8a**), we further suggest that the attentional blink is caused by a competition between the neural processes underlying the P3b wave evoked by the T1 task and those underlying the N2 wave evoked by T2. Depending on stochastic variations in the strength or duration of this P3b, T2 would either succeed or fail to enter second-stage processing. Both stochastic variations in the attentional

**Figure 6** Temporal dynamics of the cortical activity evoked by seen and unseen T2s. The graphs at right show the time courses of reconstructed cortical activation at four different sites when T2 was seen and when T2 was not seen during the attentional blink. Selected sites are circled in black on the activation maps at left, reconstructed for the seen minus unseen comparison at 300 and 436 ms after T2 (conventions as in Fig. 2). Activation at a middle temporal site on the left initially increased identically for seen and unseen T2s from ~180 to 200 ms, at which point both activation curves started to diverge. From 200 ms onward, activation was observed in inferior frontal, dorsolateral prefrontal and cingulate sites only when T2 was seen. Note that the time course of the reconstructed cingulate activity for seen T2s matches the time course of the P3a wave that was solely observed for seen T2s.



blink<sup>19</sup> and the role of N2-P3 competition<sup>40,41</sup> were predicted by previous computational models of the attentional blink. Empirical support for this mechanism comes from our analysis of single-trial signal strength, which indicates that the dynamical time course of the P3b induced by the T1 task correlates with the subsequent visibility of T2 (Fig. 8b).

### Use of a continuous scale to evaluate perception

The continuous scale allows us to show that the attentional blink mainly results in an increased number of trials in which the observers respond to the target word as if it were absent, reflecting a truly 'unseen' state. However, as this scale conflates several aspects of perception, from detection to identification, further experiments will be needed to specify the content of the state that was labeled as 'seen' in the present work. Such experiments might, for instance, measure simultaneously subjective visibility ratings and the objective ability to name the word. Ongoing work from our laboratory suggests that there is a very high correlation between the seen/unseen dichotomy and the ability to name or categorize the target word (R. Gaillard and A. Delcul, personal communication). This is in accordance with a recent study showing that there is no difference between the capacity to detect or to categorize a masked object across a wide range of exposure durations<sup>42</sup>.

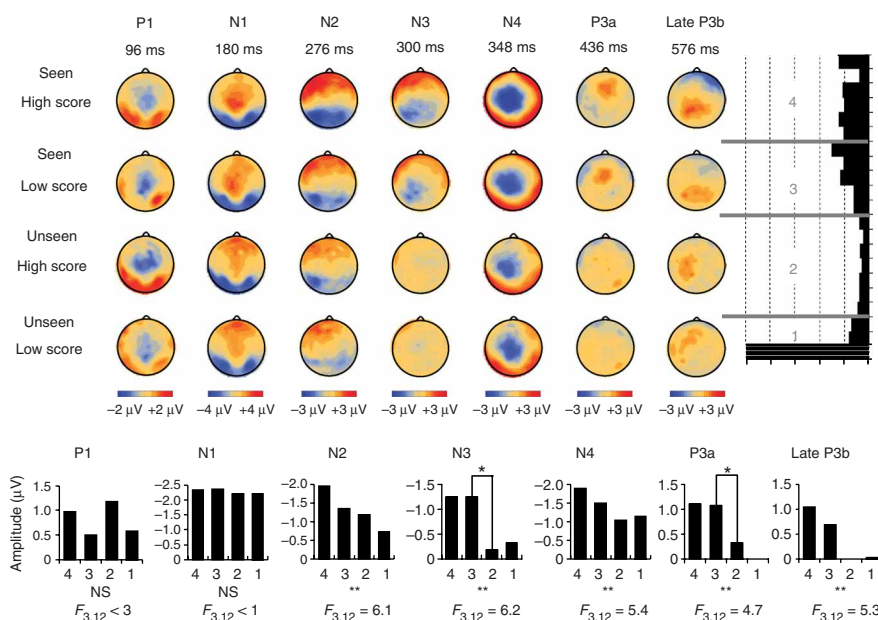
More generally, we surmise that the study of the neural basis of consciousness, which requires cross-correlation of subjective reports with objective brain measures, may greatly benefit from the use of multiple quantitative methods such as the present method for collecting phenomenological data.

### METHODS

**Participants.** Sixteen right-handed native French speakers took part in the experiment (seven women and nine men; mean age: 24, ranging from 18 to 36). All had normal or corrected-to-normal vision. All participants provided informed written consent to take part to the experiment. This study has

**Figure 7** Neural events correlating with the bimodal conscious report. Voltage maps obtained during the attentional blink when further subdividing the trials into four categories of visibility (arranged in four rows). These voltage maps are shown at various times after T2 onset (in columns). The subdivision of the scale is illustrated on the response distribution obtained during the attentional blink, represented on the right, with 100% visibility at the top and 0% visibility at the bottom (reproduced from Fig. 1). Gray lines indicate the separation between the four different trial categories used in this analysis, from the lowest visibility scores (category 1) to the highest visibility scores (category 4). (Note that separations within the seen and unseen categories varied across participants; see Methods.)

Histograms at the bottom represent, for each ERP wave, the mean amplitude obtained in the various visibility categories. Mean amplitude for each ERP wave was calculated using the electrodes and time windows identified in the previous 'seen versus unseen' analysis. Statistical significance of the main effect of visibility category is shown below each histogram (\*\*:  $P < 0.01$ ; \*:  $P < 0.05$ ; NS: not significant).



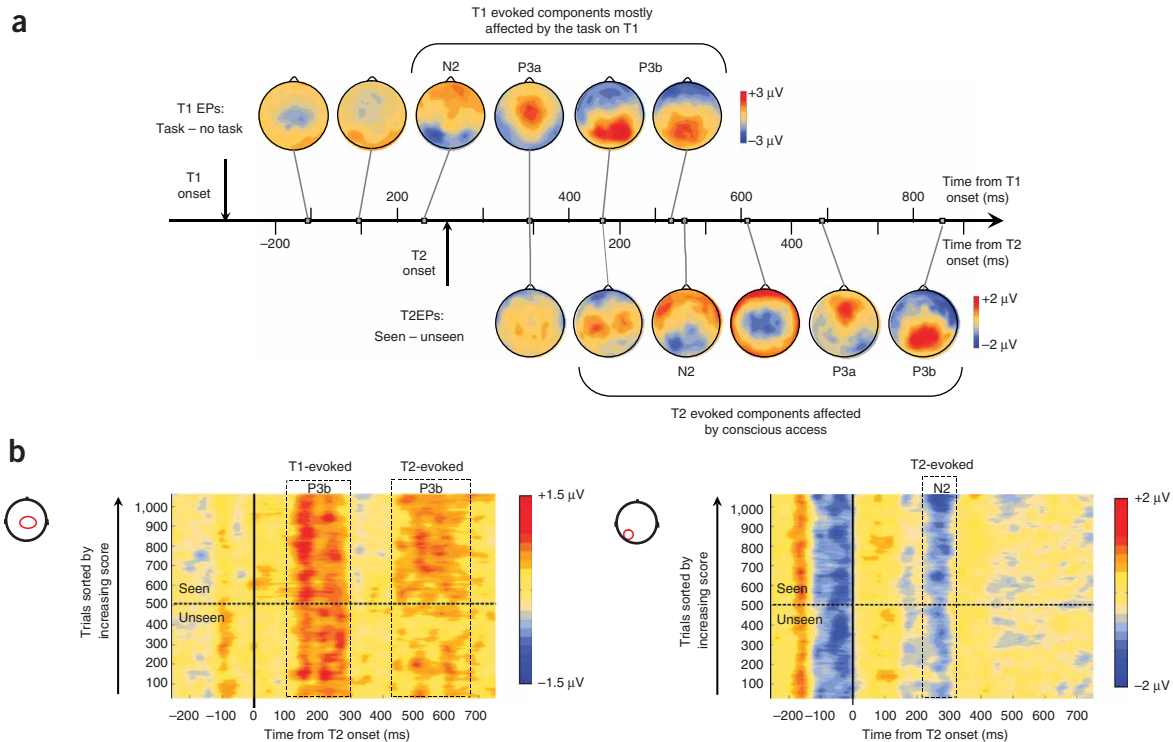


**Figure 8** Causes of the attentional blink. **(a)** Temporal relation between ERP waves evoked by the task on T1 (which causes the blink on T2) and ERP waves evoked by T2 in the seen minus unseen comparison. Voltage maps above timeline show the difference between trials with and without a task on T1 (short SOA, T2 absent), over time. Voltage maps below timeline show the ‘T2 seen’ minus ‘T2 unseen’ difference during the attentional blink (dual task, short SOA), over time. **(b)** Relation between the P3b waves evoked by T1 and the N2 and P3b waves evoked by T2, shown on a trial-by-trial basis during the attentional blink (data from all 16 participants). Note that these are nonsubtracted data; therefore, the ERPs evoked by both T1 and T2 can be observed. Each graph shows voltage recorded over a different electrode group (positions on the scalp are indicated with a red circle). In each graph, each line represents the voltage recorded for one trial in color code (positive voltage in red, negative in blue), with trials sorted according to the visibility score on the scale. For readability, voltage values were smoothed over 50 trial windows.

been approved by the CCPRB (Comité Consultatif pour la Protection des Personnes dans la Recherche Biomédicale), Hôpital de Bicêtre, Le Kremlin-Bicêtre, France.

**Design and procedure.** The stimuli were presented on a black background at the center of the computer screen (70 Hz refresh) using Expe6 software<sup>43</sup>. Each trial consisted in a simple sequence containing five items: T1 followed by a mask, and T2 (which could be present or absent) followed by two successive masks (Fig. 1). T1, T2 and the masks were each presented for 43 ms and were separated by blank screens lasting 43 ms. T1 was presented either 516 ms or 860 ms after the beginning of the trial (which started with the onset of a fixation cross). The SOA between T1 and T2 could be either short (258 ms) or long (688 ms). A central fixation cross was presented during the intervals. Targets and masks were strings of four uppercase letters presented in white and subtending  $4^\circ \times 1^\circ$  of visual angle. T1 was either ‘XOOX’ or ‘OXXO’. When T2 was present, it was a French number word: ‘DEUX’, ‘CINQ’, ‘SEPT’ or ‘HUIT’. Four white squares ( $0.5^\circ \times 0.5^\circ$  each), presented simultaneously with T2, surrounded the zone where the number word was presented. In the ‘T2 absent’ trials, the four squares were presented on an empty screen. The masks were consonant-strings, randomly generated using all consonants except Q, T and X.

In different blocks of trials, participants either performed only the subjective visibility rating on T2 (single task condition) or also performed a discrimination task on T1 (dual task condition). In both conditions, the subjective visibility judgment was performed on a continuous scale presented 715 ms after T2 onset (that is, 500 ms after the offset of the last mask). This scale took the form of a horizontal bar ( $26^\circ \times 2^\circ$ ) presented at the center of the screen, labeled ‘nothing’ at left (standing for ‘I have seen nothing at the time of T2’) and ‘maximal visibility’ at right. Participants moved a cursor on the scale by pressing two designated keys on the computer keyboard and then validated

their choice by pressing the space bar. The cursor, a vertical rectangle ( $1.2^\circ \times 2^\circ$ ), could take 21 contiguous positions on the scale by steps of 5% visibility. Its initial position was random. At the beginning of the experiment, participants were instructed to use the scale to rate the visibility of T2 as finely as possible without time pressure. They were told that the left end of the scale should be used only when they were sure that they had not seen T2. If subjects had any feeling of having seen T2, even if they were not sure, they were told to shift the cursor away from the left extremity. They were told to use the right extremity only for crisply visible T2s, and any intermediate locations to estimate the extent to which their perception of T2 was degraded relative to this maximal visibility level. Previous results have established the reliability of this procedure to measure small changes in subjective perception with small changes in the duration of masked words using pattern masking<sup>15</sup>.

In the dual-task condition only, once the participant had evaluated T2 visibility, they reported whether the central letters of T1 were ‘OO’ (T1 = ‘XOOX’) or ‘XX’ (T1 = ‘OXXO’).

After a short training, each participant performed a single-task and a dual-task session. The order of the sessions was counterbalanced across participants. In the single-task session, participants performed 32 trials per SOA  $\times$  ‘T2 present’ condition. In the dual-task session, participants performed 96 trials in the critical blink condition (T2 present at short SOA) and 48 trials in the other SOA  $\times$  ‘T2 present’ conditions. Trials with an incorrect response to T1 ( $11 \pm 5\%$ ) were discarded from subsequent behavioral and ERP analysis. ‘False positive trials’ (that is, ‘T2 absent’ trials in which subjective visibility was above 50%) were discarded from the ERP analysis (fewer than 2% of the ‘T2 absent’ trials in each condition).

**ERP methods.** ERPs were sampled at 250 Hz with a 128-electrode geodesic sensor net referenced to the vertex. We rejected voltage exceeding  $\pm 200 \mu$ V,

transients exceeding  $\pm 100$   $\mu\text{V}$ , or electrooculogram activity exceeding  $\pm 70$   $\mu\text{V}$ . The remaining trials were averaged in synchrony with T2 onset (or T1 onset for T1-evoked ERPs), digitally transformed to an average reference, band-pass filtered (0.5–20 Hz) and corrected for baseline over a 250-ms window during fixation at the beginning of the trial.

**Seen versus unseen T2s.** We identified time windows in which groups of electrodes showed a significant difference between present and seen T2s (visibility  $\geq 50\%$ ) and absent T2s, as defined by sample-by-sample *t*-tests with a criterion of  $P < 0.05$  for at least ten consecutive samples (40 ms) on at least ten electrodes. To then expand the analysis to compare all three conditions (T2 present and seen, T2 present and unseen, T2 absent) and to assess lateralization effects with a higher sensitivity, analyses of variance (ANOVAs) testing all contrasts were performed using mean voltage over the periods and groups of electrodes defined in the seen versus absent contrast (except for the P170 wave, which was identified directly on the seen versus unseen contrast). For bilateral waves, we separated left and right symmetrical groups of electrodes. Note that in the ANOVA testing for the seen versus absent contrast, main effects were expected to be significant, as the time windows and electrode groups were defined on the basis of this contrast.

**Four categories of visibility.** For each participant, we further computed the median of the response distribution within the ‘seen’ trials (visibility  $\geq 50\%$ ) and within the ‘unseen’ trials (visibility  $< 50\%$ ). Within the ‘seen’ and ‘unseen’ categories, we distinguished trials in which T2 received high visibility scores (above median) and low visibility scores (below median). We discarded from this analysis three participants for whom one of the four categories contained fewer than 6% of trials. For the other 13 participants, median visibility was  $\sim 77 \pm 11\%$  visibility for the ‘seen’ trials and  $\sim 10 \pm 10\%$  visibility for the ‘unseen’ trials. The time windows and electrode groups defined in the previous analysis (seen versus unseen T2s) were used for the ANOVAs testing all contrasts in this analysis.

**Causes of the blink: ERPs evoked by the task on T1.** We contrasted the ERPs evoked by T1 when participants did or did not perform a task on T1 (dual-versus single-task), at short SOA in the ‘T2 absent’ condition. The different time windows and electrode groups for the analysis were defined on the dual-versus single-task contrast (same criterion as above), except for the P1 and N1 waves evoked by T1, which were clearly identifiable on the nonsubtracted ERPs.

**Causes of the blink: trial-by-trial analysis.** For all 16 participants, and trial by trial, we computed the mean voltage over a group of electrodes (parietocentral) capturing the T1-evoked P3b, as defined in the ‘dual- versus single-task’ analysis, and over a group of electrodes (left temporal) capturing the T2-evoked N2, as defined in the ‘seen versus unseen T2’ analysis. Note that electrodes belonging both to the P3b and N2 groups were discarded from the P3b electrode group to minimize contamination. Trial-by-trial voltages for both electrode groups were plotted as a function of T2 visibility on the scale (Fig. 8b). Using unpaired *t*-tests, we then compared the T1-evoked P3b in the trials where T2 would later be seen or unseen. This comparison was made over an early time window (358–458 ms after T1; that is, 100–200 ms after T2) and over a late time window (462–558 ms after T1; that is, 204–300 ms after T2).

**Differences in topographies.** The statistical tool used to assess differences in topographies was provided by C. Michel (Geneva University Medical School). Voltage maps were first normalized for global field power. The dissimilarity between two conditions was then computed as the root mean square of the differences between those two conditions at each electrode site (global map dissimilarity<sup>44</sup>). Statistical significance of the dissimilarity for each sample was tested using bootstrap based on 8,000 random permutations of both conditions within subjects. Topographies obtained in two conditions were considered to be significantly different if they differed at  $P < 0.05$  over more than ten consecutive samples.

**Source modeling.** Cortical current density mapping was obtained using a distributed model consisting of 10,000 current dipoles. Dipole locations and orientations were constrained to the cortical mantle of a generic brain model built from the standard brain of the Montreal Neurological Institute using the

BrainSuite software package (<http://brainsuite.usc.edu/>). This head model was then warped to the standard geometry of the EEG sensor net<sup>45</sup>. The warping procedure and all subsequent source analysis and surface visualization were processed with the BrainStorm software package (<http://neuroimage.usc.edu/brainstorm>). EEG forward modeling was computed with an extension to EEG of the overlapping-spheres analytical model<sup>46</sup>. Cortical current maps were computed from the EEG time series using a linear inverse estimator (weighted minimum-norm current estimate (WMNE); see ref. 47 for a review).

*Note: Supplementary information is available on the Nature Neuroscience website.*

#### ACKNOWLEDGMENTS

We thank C. Michel for helping us in the analysis of topographical differences, M. Sigman for helping us generate the movie and J.-P. Changeux, P. Coiron, V. Izard and M. Sigman for useful comments. We are also grateful to R.M. Leahy, J.C. Mosher, F. Darvas and D. Pantazis from the BrainStorm and BrainSuite projects. This study was supported by INSERM (Institut National de la Santé et de la Recherche Médicale) and a centennial fellowship from the McDonnell Foundation to S.D.

#### COMPETING INTERESTS STATEMENT

The authors declare that they have no competing financial interests.

Published online at <http://www.nature.com/natureneuroscience/>  
Reprints and permissions information is available online at <http://npg.nature.com/reprintsandpermissions/>

- Dehaene, S. *et al.* Cerebral mechanisms of word masking and unconscious repetition priming. *Nat. Neurosci.* **4**, 752–758 (2001).
- Moutoussis, K. & Zeki, S. The relationship between cortical activation and perception investigated with invisible stimuli. *Proc. Natl. Acad. Sci. USA* **99**, 9527–9532 (2002).
- Grill-Spector, K., Kushnir, T., Hendler, T. & Malach, R. The dynamics of object-selective activation correlate with recognition performance in humans. *Nat. Neurosci.* **3**, 837–843 (2000).
- Bar, M. *et al.* Cortical mechanisms specific to explicit visual object recognition. *Neuron* **29**, 529–535 (2001).
- Shulman, G.L., Ollinger, J.M., Linenweber, M., Petersen, S.E. & Corbetta, M. Multiple neural correlates of detection in the human brain. *Proc. Natl. Acad. Sci. USA* **98**, 313–318 (2001).
- Vuilleumier, P. *et al.* Neural fate of seen and unseen faces in visuospatial neglect: a combined event-related functional MRI and event-related potential study. *Proc. Natl. Acad. Sci. USA* **98**, 3495–3500 (2001).
- Marois, R., Yi, D.J. & Chun, M.M. The neural fate of consciously perceived and missed events in the attentional blink. *Neuron* **41**, 465–472 (2004).
- Beck, D.M., Rees, G., Frith, C.D. & Lavie, N. Neural correlates of change detection and change blindness. *Nat. Neurosci.* **4**, 645–650 (2001).
- Pins, D. & Ffytche, D. The neural correlates of conscious vision. *Cereb. Cortex* **13**, 461–474 (2003).
- Dehaene, S., Kerszberg, M. & Changeux, J.P. A neuronal model of a global workspace in effortful cognitive tasks. *Proc. Natl. Acad. Sci. USA* **95**, 14529–14534 (1998).
- Baars, B.J. *A Cognitive Theory of Consciousness* (Cambridge Univ. Press, Cambridge, 1989).
- Rees, G., Kreiman, G. & Koch, C. Neural correlates of consciousness in humans. *Nat. Rev. Neurosci.* **3**, 261–270 (2002).
- Broadbent, D.E. & Broadbent, M.H. From detection to identification: response to multiple targets in rapid serial visual presentation. *Percept. Psychophys.* **42**, 105–113 (1987).
- Raymond, J.E., Shapiro, K.L. & Arnell, K.M. Temporary suppression of visual processing in an RSVP task: an attentional blink? *J. Exp. Psychol. Hum. Percept. Perform.* **18**, 849–860 (1992).
- Sergent, C. & Dehaene, S. Is consciousness a gradual phenomenon? Evidence for an all-or-none bifurcation during the attentional blink. *Psychol. Sci.* **15**, 720–728 (2004).
- Luck, S.J., Vogel, E.K. & Shapiro, K.L. Word meanings can be accessed but not reported during the attentional blink. *Nature* **383**, 616–618 (1996).
- Vogel, E.K., Luck, S.J. & Shapiro, K.L. Electrophysiological evidence for a postperceptual locus of suppression during the attentional blink. *J. Exp. Psychol. Hum. Percept. Perform.* **24**, 1656–1674 (1998).
- Kranciach, C., Debener, S. & Engel, A.K. Event-related potential correlates of the attentional blink phenomenon. *Brain Res. Cogn. Brain Res.* **17**, 177–187 (2003).
- Dehaene, S., Sergent, C. & Changeux, J.P. A neuronal network model linking subjective reports and objective physiological data during conscious perception. *Proc. Natl. Acad. Sci. USA* **100**, 8520–8525 (2003).
- Thom, R. *Stabilité Structurelle et Morphogénèse* (InterEditions, Paris, 1972).
- Dehaene, S. & Changeux, J.P. Ongoing spontaneous activity controls access to consciousness: a neuronal model for inattention blindness. *PLoS Biol.* **3**, e141 (2005).
- Chun, M.M. & Potter, M.C. A two-stage model for multiple target detection in rapid serial visual presentation. *J. Exp. Psychol. Hum. Percept. Perform.* **21**, 109–127 (1995).

23. McArthur, G., Budd, T. & Michie, P. The attentional blink and P300. *Neuroreport* **10**, 3691–3695 (1999).
24. Shapiro, K.L., Caldwell, J. & Sorensen, R.E. Personal names and the attentional blink: a visual 'cocktail party' effect. *J. Exp. Psychol. Hum. Percept. Perform.* **23**, 504–514 (1997).
25. Devlin, J.T., Jamison, H.L., Matthews, P.M. & Gonnerman, L.M. Morphology and the internal structure of words. *Proc. Natl. Acad. Sci. USA* **101**, 14984–14988 (2004).
26. Kranczioch, C., Debener, S., Schwarzbach, J., Goebel, R. & Engel, A.K. Neural correlates of conscious perception in the attentional blink. *Neuroimage* **24**, 704–714 (2005).
27. Super, H., Spekreijse, H. & Lamme, V.A. Two distinct modes of sensory processing observed in monkey primary visual cortex (V1). *Nat. Neurosci.* **4**, 304–310 (2001).
28. Lamme, V.A., Zipser, K. & Spekreijse, H. Masking interrupts figure-ground signals in V1. *J. Cogn. Neurosci.* **14**, 1044–1053 (2002).
29. Ress, D. & Heeger, D.J. Neuronal correlates of perception in early visual cortex. *Nat. Neurosci.* **6**, 414–420 (2003).
30. Marois, R., Chun, M.M. & Gore, J.C. Neural correlates of the attentional blink. *Neuron* **28**, 299–308 (2000).
31. Pammer, K. *et al.* Visual word recognition: the first half second. *Neuroimage* **22**, 1819–1825 (2004).
32. Marinkovic, K. *et al.* Spatiotemporal dynamics of modality-specific and supramodal word processing. *Neuron* **38**, 487–497 (2003).
33. Feinstein, J.S., Stein, M.B., Castillo, G.N. & Paulus, M.P. From sensory processes to conscious perception. *Conscious. Cogn.* **13**, 323–335 (2004).
34. Gross, J. *et al.* Modulation of long-range neural synchrony reflects temporal limitations of visual attention in humans. *Proc. Natl. Acad. Sci. USA* **101**, 13050–13055 (2004).
35. Halgren, E., Marinkovic, K. & Chauvel, P. Generators of the late cognitive potentials in auditory and visual oddball tasks. *Electroencephalogr. Clin. Neurophysiol.* **106**, 156–164 (1998).
36. Lumer, E.D., Friston, K.J. & Rees, G. Neural correlates of perceptual rivalry in the human brain. *Science* **280**, 1930–1934 (1998).
37. Rees, G., Russell, C., Frith, C.D. & Driver, J. Inattention blindness versus inattentional amnesia for fixated but ignored words. *Science* **286**, 2504–2507 (1999).
38. Saunders, P.T. *An Introduction to Catastrophe Theory* (Cambridge Univ. Press, Cambridge, 1980).
39. Wickens, C., Kramer, A., Vanasse, L. & Donchin, E. Performance of concurrent tasks: a psychophysiological analysis of the reciprocity of information-processing resources. *Science* **221**, 1080–1082 (1983).
40. Taylor, J.G. Breakthrough to awareness: a preliminary neural network model of conscious and unconscious perception in word processing. *Biol. Cybern.* **75**, 59–72 (1996).
41. Fragopanagos, N.F., Kockelkoren, S. & Taylor, J.G. A neurodynamic model of the attentional blink. *Brain Res. Cogn. Brain Res.* (in the press).
42. Grill-Spector, K. & Kanwisher, N. Visual recognition: as soon as you know it is there, you know what it is. *Psychol. Sci.* **16**, 152–160 (2005).
43. Pallier, C., Dupoux, E. & Jeannin, X. Expe5: an expandable programming language for on-line psychological experiments. *Behav. Res. Methods Instrum. Comput.* **29**, 322–327 (1997).
44. Lehmann, D. & Skrandies, W. Reference-free identification of components of checkerboard-evoked multichannel potential fields. *Electroencephalogr. Clin. Neurophysiol.* **48**, 609–621 (1980).
45. Darvas, F., Ermer, J.J., Mosher, J.C. & Leahy, R.M. Generic head models for atlas-based EEG source analysis. *Hum. Brain Mapp.*, published online 21 July 2005 (doi: 10.1002/hbm.20171).
46. Huang, M.X., Mosher, J.C. & Leahy, R.M. A sensor-weighted overlapping-sphere head model and exhaustive head model comparison for MEG. *Phys. Med. Biol.* **44**, 423–440 (1999).
47. Baillet, S., Mosher, J.C. & Leahy, R.M. Electromagnetic brain mapping. *IEEE Signal Process. Mag.* **18**, 14–30 (2001).